Short Papers

Analysis of a General Coaxial-Line/Radial-Line Region Junction

R. B. Keam and A. G. Williamson

Abstract—**A general analysis of a coaxial line/radial-line region junction is presented for the case where the centre conductor is sheathed in a dielectric and extends the full width between two parallel metal plates. Expressions for the current distribution and the admittance of the junction are presented. Two example environments are considered, a rectangular waveguide and a base entrant cylindrical cavity, although the technique may be used for other environments. Comparison of theoretical and experimental results for these two cases show the theory to be very accurate.**

I. Introduction

Junctions between coaxial-line and other transmission-line systems find wide application in a variety of microwave devices. Such transitions include coaxial-line to rectangular waveguide, and coaxial-line power combiners and dividers. Until recently much of the design of these devices has been based on empirical knowledge, based on "trial and error" techniques. It would be a great saving in time and expense to have analytic models for these junctions to aid design. The analysis should be based on a model closely related to the physical situation, and should not need empirical factors which can only be obtained after extensive experimental measurements. The type of junction considered here is that where the coaxial-line center conductor extends the full width between two metal plates. The region between the two metal plates is considered to be a "radial-line" type environment, and examples of this include a coaxial-line entering through the broad wall of a rectangular waveguide, and a coaxial-line entering through the flat face of a cylindrical cavity. The radial-line case (where the top and bottom metal plates are infinite in extent) has been considered by Otto [1], and the rectangular waveguide case has been considered by Williamson [2]. These analyses have lead to accurate results for the current distribution on the center conductor and the input admittance as seen at the coaxial-line input, as well as equivalent circuit representations [3]. Until recently [4] little attention has been devoted to the analysis of sheathed junctions. The analysis presented here includes the sheathed junction case in a generic solution which may be applied to a wide range of junctions.

In this paper the method used in [1], [2] is extended to include the case where the center post in the radial-line environment is completely surrounded by a homogeneous dielectric sheath. It is shown that the method may be generalized to any radial-line type environment and, by way of example, the coaxial-line to cylindrical cavity junction is considered. Thus, the actual coaxial-line section of the junction may be treated as a functional block. The only additional parameter required when considering a wide range of possible environments is a factor which takes into account the environment external to the junction region.

Manuscript received December 17, 1991; revised June 25, 1992.

The authors are with the Department of Electrical and Electronic Engineering, University of Auckland, Private Bag 92019, Auckland, New Zealand.

IEEE Log Number 9205453.

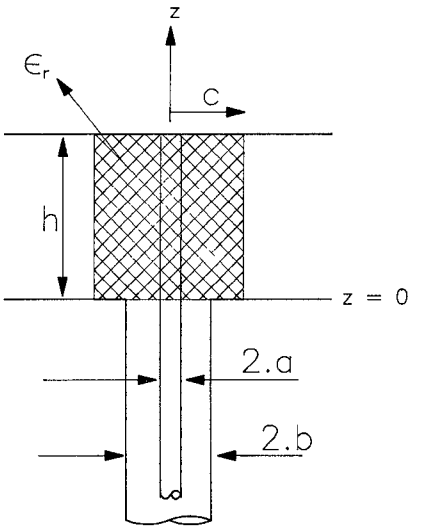

Fig. 1. A general coaxial-line to radial-line junction.

Finally, a comparison of theoretical and experimental results is given which shows the technique to be very accurate.

II. Theory

Consider the junction shown in Fig. 1 in which the center conductor of the coaxial-line, of radius $r = a$, extends the full width between the top and bottom plates, of separation h. The outer conductor of the coaxial-line, and hence the aperture in the radial-line region is of radius $r = b$. In the radial-line region the center conductor is surrounded by a homogeneous, lossless dielectric sheath of relative permittivity ε_r and radius $r = c$. In the analysis presented here it is assumed that the region for $r > c$ is filled with a lossless air dielectric (though extension to include other homogeneous, lossless dielectrics is straightforward), and that the fields may be average matched at the $r = c$ boundary.

It is assumed in the analysis that the junction is driven from the coaxial-line, and that the dimensions of the coaxial-line are such that only the TEM mode can propagate in the line at the frequency of interest. It is also assumed that all metal surfaces are perfectly conducting, and that the fields have a time dependence of $e^{j\omega t}$.

It has been shown elsewhere, using image theory [2], that the fields of the junction problem are equivalent to those of an infinite cylindrical antenna (of radius $r = a$) excited by an infinite series of magnetic frills spaced at intervals of $2h$ along it. This automatically satisfies the boundary conditions on the top and bottom metal surfaces. The fields in one "cell" ($0 < z < h$) of the problem are equivalent to those in the radial-line region. It has also been shown that the analysis of this equivalent problem is assisted by first considering a similar situation with only one magnetic frill located at $z = 0$. The solution to the problem may be simplified by taking the spatial Fourier Transform [1] with respect to the z-axis, considering an antenna with only one magnetic frill at $z = 0$, and solving firstly for the (FT) fields and current distribution.

If the current distribution on the single-frill antenna is given by $I^*(z)$ then, by the principle of superposition, the current distribution

on the infinite frill antenna, $I(z)$, is easily shown to be given by

$$I(z) = \sum_{m=-\infty}^{\infty} I^*(z + 2mh) \tag{1}$$

which can be shown, by Poisson's Summation Formula to be

$$I(z) = \frac{1}{2h}\left\{\mathcal{I}(\alpha = 0) + 2\sum_{m=1}^{\infty} \mathcal{I}(\alpha = m\pi/h)\cos(m\pi z/h)\right\} \tag{2}$$

where $\mathcal{I}(\alpha)$ is the Fourier transform with respect to z of $I^*(z)$ (Fourier transformed quantities are henceforth given in script), and

$$\mathcal{I}(\alpha) = \int_{-\infty}^{+\infty} I^*(z)e^{-j\alpha z}\,dz \tag{3}$$

The use of Poisson's Summation Formula in (2) means that superposition and Fourier transform inversion have been applied in one step.

The analysis of the problem may be considered in terms of three regions; $a < r < b$ inside the frill region; $b < r < c$ outside the frill but inside the dielectric sheath; and $r > c$ outside the sheath. The (FT) fields within the dielectric sheath ($a < r < c$) are assumed to be axially-symmetric as a simplification. Thus the current distribution on the center post is also assumed to be axially-symmetric (this is reasonable for an electrically thin center post). This assumption is also reasonable for the calculation of admittance since the admittance is related to the average fields in the aperture ($a < r < b$) region. Whilst the fields outside the sheath region (in the "radial-line" environment) may have θ variation for some situations, they will be average matched at the dielectric interface at $r = c$. The (FT) fields in the two dielectric regions are given by

$$\begin{aligned}\mathcal{E}_z = {} & \frac{-q'^2\eta'}{j2\pi k'}\mathcal{I}(\alpha)I_0(q'a)K_0(q'r) \\ & - \frac{2}{\ln(b/a)}\{I_0(q'r)K_0(q'b) \\ & - I_0(q'a)K_0(q'r)\} + AI_0(q'r) \qquad \text{for } a \le r \le b\end{aligned} \tag{4}$$

$$\begin{aligned}\mathcal{H}_\theta = {} & \frac{q'}{2\pi}\mathcal{I}(\alpha)I_0(q'a)K_1(q'r) \\ & + \frac{j2k'}{q'\eta'\ln(b/a)}\left\{\frac{1}{q'r} - I_1(q'r)K_0(q'b) - I_0(q'b)K_1(q'r)\right\} \\ & + \frac{jk'}{q'\eta'}AI_1(q'r) \qquad \text{for } a \le r \le b\end{aligned} \tag{5}$$

and

$$\begin{aligned}\mathcal{E}_z = {} & \frac{-q'^2\eta'}{j2\pi k'}\mathcal{I}(\alpha)I_0(q'a)K_0(q'r) \\ & - \frac{2}{\ln(b/a)}K_0(q'r)I'_{ba} + AI_0(q'r) \qquad \text{for } b \le r \le c\end{aligned} \tag{6}$$

$$\begin{aligned}\mathcal{H}_\theta = {} & \frac{q'}{2\pi}\mathcal{I}(\alpha)I_0(q'a)K_1(q'r) \\ & + \frac{j2k'}{q'\eta'\ln(b/a)}K_1(q'r)I'_{ba} + \frac{jk'}{q'\eta'}AI_1(q'r) \quad \text{for } b \le r \le c\end{aligned} \tag{7}$$

whilst the fields in the region outside the sheath are of the form;

$$\mathcal{E}_z = E(K_0(qr) + SI_0(qr) + e_p\cos p\theta) \qquad \text{for } r \ge c \tag{8}$$

$$\mathcal{H}_\theta = \frac{-jk}{q\eta}E\left(K_1(qr) - SI_1(qr) + \sum_{p=-\infty}^{\infty} h_p\cos p\theta\right) \qquad \text{for } r \ge c \tag{9}$$

Since we will average match the fields at $r = c$, we will not need to determine the e_p and h_p coefficients. I_0 and I_1 are modified Bessel functions of the first kind and are associated with inward travelling waves, and K_0 and K_1 are modified Bessel functions of the second kind and are associated with outward travelling waves. Also k', η', and k, η are the wave numbers and intrinsic impedances within and outside the dielectric (dashed symbols refer to quantities within the dielectric region), $I'_{ba} = I_0(q'b) - I_0(q'a), q = \sqrt{\alpha^2 - k^2}$, and $q' = \sqrt{\alpha^2 - k'^2}$.

The terms involving the constant A (to be determined by a suitable boundary condition) are associated with an inward reflected wave from the dielectric interface and the terms involving the constant S (henceforth referred to as the "environment factor") are related to the average of the electric field of the inward travelling wave due to the environment outside the dielectric sheath. Note that (4)–(7) already satisfy the condition that the fields are continuous across the $r = b$ interface.

If the boundary conditions, that $\mathcal{E}_z(r = a) = 0$, and the average values with respect to θ of both $\mathcal{E}_z$ and $\mathcal{H}_\theta$ are continuous across the surface $r = c$ are applied, the result is (10) at the bottom of the page, where $K'_{ba} = K_0(q'b) - K_0(q'a), S_0 = K_0(qc) + S.I_0(qc)$,and $S_1 = K_1(qc) - S.I_1(qc)$.

This may be substituted into (2) to give the current distribution on the center post. If S is set to zero (i.e., the radial-line case) and ε_r is set to unity (i.e., no sheath) then the result in (10) reduces to that given by Otto [1].

It has been shown [1] that the admittance looking into the junction from the coaxial-line at $z = 0$ is given by

$$Y = \frac{1}{2h}\left\{\mathcal{Y}(\alpha = 0) + 2\sum_{m=1}^{\infty}\mathcal{Y}(\alpha = m\pi/h)\right\} \tag{11}$$

where

$$\mathcal{Y}(\alpha) = \frac{2\pi}{\eta\ln(b/a)}\int_a^b \mathcal{H}_\theta(\alpha, 0)\,dr \tag{12}$$

Using the results for $\mathcal{I}(\alpha)$ and (5), (13) is shown at the bottom of the next page. For $S = 0$ and $\varepsilon_r = 1$, this result also reduces to that given in [1].

In order to find the solution for any other type of region outside the sheath, all that is required is the environment factor S. This factor is the average with respect to angular variation, at $r = c$, of the inward travelling wave caused by the environment external to the dielectric, with the fields in the dielectric being assumed to be axially symmetric. The actual fields outside the sheath are not required to be axially symmetric.

Two interesting examples follow, firstly that where there is a short circuit located in the radial-line at a radius $r = d$ (i.e., a cylindrical cavity), and secondly the coaxial-line/rectangular waveguide junction.

$$\begin{aligned}\mathcal{I}(\alpha) = {} & \frac{-j4\pi k'}{q'^2\eta'\ln(b/a)} \\ & \times \frac{q'S_1(K_0(q'c)I'_{ba} - I_0(q'c)K'_{ba}) - q\varepsilon_r S_0(I_1(q'c)K'_{ba} + K_1(q'c)I'_{ba})}{q'S_1(K_0(q'c)I_0(q'a) - I_0(q'c)K_0(q'a)) - q\varepsilon_r S_0(I_1(q'c)K_0(q'a) + K_1(q'c)I_0(q'a))}\end{aligned} \tag{10}$$

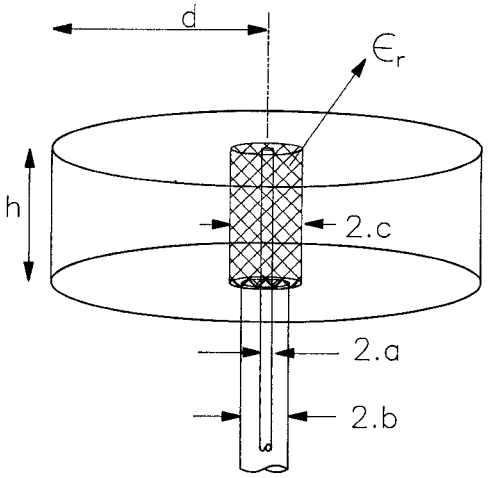

Fig. 2. A coaxial-line to cylindrical cavity junction.

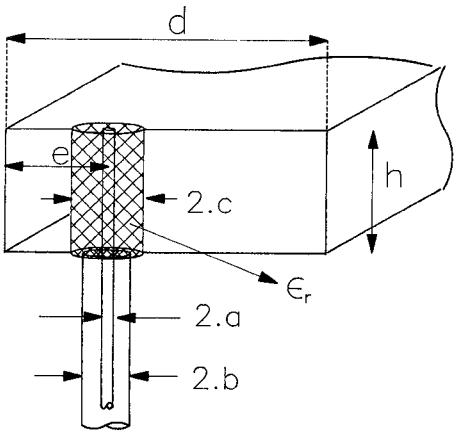

Fig. 3. Sectional view of a coaxial-line/rectangular waveguide junction.

III. Cylindrical Cavity Junction

Consider Fig. 2, the case where a short circuit is located in the radial-line at a radius $r = d$ (where $d > c$). The (FT) electric field in the region of the sheath ($c < r < d$) is axially symmetric, but has two components; an outward travelling wave radiated by the junction, and an inward travelling wave reflected by the cavity wall at $r = d$. By applying the condition that the electric field at $r = d$ must be zero it is easy show that the environment factor S is;

$$S = -\frac{K_0(qd)}{I_0(qd)}. \tag{14}$$

The solution for the current distribution and input admittance may be obtained for the case of no dielectric sheath, simply by substituting $\varepsilon_r = 1$ into all of the relevant equations.

IV. Rectangular Waveguide

Consider Fig. 3, a rectangular waveguide of cross sectional dimensions d and h, where $d > h$. The coaxial-line enters the waveguide through the broad wall at a distance e from the side wall. The fields outside of the sheath region are now functions of both r and θ. All that is now required is to find the total average (FT) electric field external to the dielectric boundary, and hence the environment factor, S.

Using image theory to satisfy the boundary conditions on the side walls [2], the problem can be shown to be equivalent to an infinite array of parallel, sheathed junctions. It is assumed that each junction in the array is radiating axially symmetrical about its own center, but that the total field at any point is a function of both r and θ. The total field due to all the junctions is to be summed external to the $n = 0$ junction sheath, and then average matched [2] to the fields within the $n = 0$ junction sheath. Thus the contribution to the (FT) electric field from the nth junction is

$$\mathcal{E}_z^n = EK_0(qR_n) \tag{15}$$

where R_n is the radius relative to the center of the nth post's own axis. The addition theorem for modified Bessel functions [5] may be used to show that;

$$K_0(qR_n) = \sum_{p=-\infty}^{\infty} K_p(qx_n) \cdot I_p(qr)(-1)^p \cos(p\theta) \quad x_n > r \tag{16}$$

where r is the radius relative to the $n = 0$ junction, x_n is the distance between the nth junction and "parent" junction, and I_p and K_p are pth order modified Bessel functions of the first and second kind. This gives the fields due to the other junctions, relative to the $n = 0$ junction, as axially varying, inward travelling waves. The average (FT) electric field due to the nth junction, just outside of the parent junction's sheath is

$$\mathcal{E}_z^{\text{average}} = EK_0(qx_n)I_0(qr) \tag{17}$$

and so the total average field due to all the junctions, relative to the $n = 0$ junction, is

$$\mathcal{E}_z^{\text{total}} = EK_0(qr) + EI_0(qr) \cdot \left\{ \sum_{\substack{n=-\infty \\ n\neq 0}}^{\infty} K_0(2|n|qd) - \sum_{n=-\infty}^{\infty} K_0(2|n + e/d|qd) \right\} \tag{18}$$

It can be seen by comparing (18) with (8), that the environment factor S is given by

$$S = \sum_{\substack{n=-\infty \\ n\neq 0}}^{\infty} K_0(2|n|qd) - \sum_{n=-\infty}^{\infty} K_0(2|n + e/d|qd) \tag{19}$$

which is equivalent to the "array factor" derived by Williamson [2]. Equation (19) may now be substituted back into (10) and (13) to give the current distribution on the junction's center conductor and the admittance looking into the junction at the coaxial-line port.

Upon substituting $\varepsilon_r = 1$ (i.e., no sheath) the results for both the current distribution and admittance reduce to that given by

$$\mathcal{Y}(\alpha) = \frac{j4\pi k'}{q'^2\eta' \ln^2(b/a)} \left\{ \ln(b/a) + (I_0(q'a)K_0(q'b) - I_0(q'b)K_0(q'a)) \times \frac{q'S_1(K_0(q'c)I_0(q'b) - K_0(q'b)I_0(q'c)) - q\varepsilon_r S_0(K_1(q'c)I_0(q'b) + K_0(q'b)I_1(q'c))}{q'S_1(K_0(q'c)I_0(q'a) - K_0(q'a)I_0(q'c)) - q\varepsilon_r S_0(K_1(q'c)I_0(q'a) + K_0(q'a)I_1(q'c))} \right\} \tag{13}$$

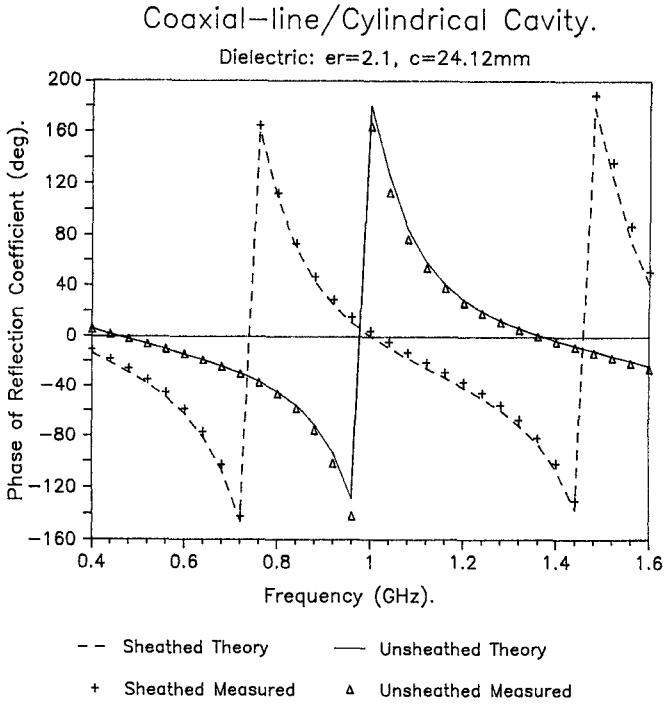

Fig. 4. Phase of reflection coefficient of the coaxial-line/cylindrical cavity junction for both the sheathed and unsheathed cases.

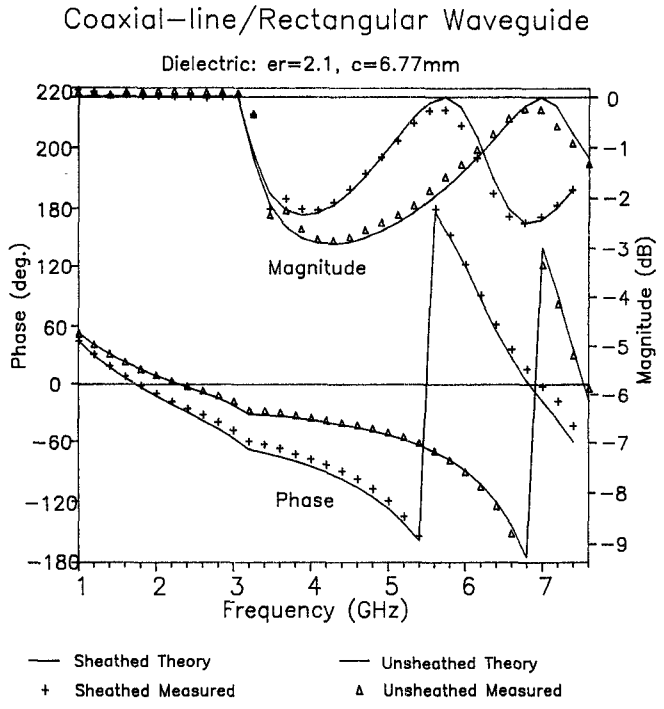

Fig. 5. Magnitude and phase of reflection coefficient of the coaxial-line/rectangular waveguide junction for both the sheathed and unsheathed cases.

Williamson in [2]. It is worth noting that, while Williamson allowed the total field to vary axially within the coaxial aperture, the integration for the admittance effectively averages the fields within the aperture. Thus both methods yields the same results for the case of no sheath.

V. Theoretical and Experimental Comparison

It is appropriate at this stage to demonstrate the accuracy of the theory by comparing theoretical predictions with experimental measurements. The reflection coefficient at the coaxial aperture plane has been measured for both the rectangular waveguide junction, and cylindrical cavity junction and compared to the results obtained from the admittance expression. For both cases $50\,\Omega$ coaxial-line was used with dimensions of $a = 1.525$ mm and $b = 3.50$ mm.

In Fig. 4 theoretical and experimental results are shown for the phase of the reflection coefficient for the coaxial-line/cylindrical cavity junction for both the sheathed and unsheathed cases (the magnitude of the reflection coefficient is, of course, equal to one). The dimensions of the cavity were $d = 41.0$ mm and $h = 150$ mm. The dielectric was Teflon with a radius $c = 24.12$ mm and a relative permittivity of $\varepsilon_r = 2.1$. Clearly the agreement between theoretical and experimental results is excellent.

For the unsheathed case the first resonance would occur when $kh = \pi$, at 1 GHz, and for a completely dielectrically filled cavity the first resonance would occur when $k'h = \pi$, at 690 MHz. The resonant frequency for the sheathed case is a function of the sheath radius, and for the case shown, occurred at 720 MHz. Thus, at frequencies between 690 MHz and 1 GHz, there are two outwardly propagating modes within the sheath but only one in the main section of the cavity.

In Fig. 5 theoretical and experimental results are given for the magnitude and phase of the reflection coefficient for the coaxial-line/rectangular waveguide junction. The results for the case where there is no dielectric sheath has already been extensively investigated [2], and found to be very accurate. In the study presented here, the dimensions of the rectangular waveguide were $d = 48$ mm and $h = 22$ mm, and the dielectric was Teflon, with a radius $c = 6.77$ mm and a relative permittivity $\varepsilon_r = 2.1$. It can be seen that again there is excellent agreement between the theoretical and experimental results below cutoff and in the range 3 to 6 GHz where there is only one propagating mode, and also above 6 GHz. The model places no restriction on the number of propagating modes, but above 6 GHz the VSWR of the waveguide terminations used is unknown.

The average matching approximation at $r = c$ was applied in the rectangular waveguide junction case (the fields are axially symmetric in the coaxial-line to cylindrical cavity case considered). Clearly this approximation would be very accurate for an electrically small core region, but would be less satisfactory, and thus less accurate, for electrically larger cases. Note however, that for the case considered here excellent accuracy was obtained even when the dielectric region was approximately one quarter of the guide width (corresponding to $c \approx \lambda/8$ at 6 GHz).

VI. Conclusion

The analysis of a coaxial-line junction, where the center conductor extends the full width between two parallel metal plates and is completely surrounded by a dielectric sheath, has been presented. Expressions for the current distribution on the post, and input admittance have been given.

The analysis involves expressions for the fields which accounted for the coaxial aperture, reflections from the dielectric interface, and inward travelling waves reflected from the surrounding environment. The junction is then considered as a functional block which only requires one factor to account for the external environment. This technique can be applied to a wide range of external radial-line type environments. Two such environments, the cylindrical cavity, and the rectangular waveguide have been considered here and a comparison between theoretical and experimental results shows the method to be very accurate.

REFERENCES

[1] D. V. Otto, "The admittance of cylindrical antennas driven from a coaxial-line," *Radio Sci.*, vol. 2, pp. 1031–1042, 1967.

[2] A. G. Williamson, "Analysis and modelling of a coaxial-line/rectangular waveguide junction," *IEEE Proc. H, Microwaves, Opt. Antennas*, vol. 129, no. 5, pp. 262–270, 1982.

[3] ——, "Radial-line/coaxial-line junctions: analysis and equivalent circuits," *Int. J Electronics*, vol. 5, no. 1, pp. 91–104, 1985.

[4] M. E. Bialkowski, "Analysis of a coaxial-to-waveguide adaptor incorporating a dielectric coated probe." *Microwave Guided Wave Lett.*, vol. 1, no. 8, pp. 211–214.

[5] G. N. Watson, *A Treatise on the Theory of Bessel Functions*. London: Cambridge University Press, 1966.

A Rigorous Analysis of a Shielded Microstrip Asymmetric Step Discontinuity

C. N. Capsalis, N. K. Uzunoglu,
C. P. Chronopoulos, and Y. D. Sigourou

***Abstract*—In this paper microstrip asymmetric step discontinuities are analyzed using a mode-matching technique leading to the frequency-dependent characteristics of the structure. On both sides of the discontinuity the fields are expanded in terms of the normal even and odd hybrid modes of shielded microstrip lines, taking into account not only the propagating modes but also higher order even and odd modes, which are evanescent-type waves. The propagation constants of the even and odd hybrid modes are computed using a previously developed method. Then a mode-matching technique is applied in order to obtain the reflection and transmission coefficients of the discontinuity. Numerical results are also given for several asymmetric step discontinuities.**

I. INTRODUCTION

Modelling of discontinuities in microstrip lines is highly important in analyzing the behavior of microwave and millimeter wave circuits.

A commonly encountered discontinuity structure in microstrip lines is the asymmetric abrupt change in strip line width, which can be employed in low pass filters, quarter-wavelength transformers and generally in a wide range of microwave circuits. In that sense it is very important to develop analytical techniques to treat this discontinuity problem, especially in high frequencies (above 10 GHz) where the lumped C and L description becomes less and less valid.

Microstrip discontinuity problems have been treated in the past by several authors [1]–[8]. Several comprehensive reviews on this matter are also presented in books [9]–[12]. The unshielded asymmetric microstrip step discontinuity is studied in [2], where a magnetic-wall model is employed. However, a full-wave analysis might be required in order to describe efficiently the discontinuity behavior at very high frequencies.

In this paper the concepts of the mode-matching techniques are employed in order to formulate a full-wave analysis of the boundary condition problem associated with the asymmetric microstrip step discontinuity. The fields on both sides of the discontinuity interface are expanded in terms of both even and odd hybrid modes. The characteristics of these modes are determined by using an analysis similar to [13] by Mittra and Itoh, which determined the dispersion characteristics of microstrip lines.

Then an efficient mode-matching procedure is developed by using products involving the orthogonal functions of both microstrip lines.

The technique used in this paper is similar to that developed previously by the authors [14] but now odd symmetry modes are taken into account in order to treat the asymmetric step microstrip discontinuities.

In the following analysis the time dependence of field quantities is assumed to be $\exp(j\omega t)$ and is suppressed throughout the analysis.

Manuscript received March 12, 1991; revised June 15, 1992.

The authors are with the Department of Electrical Engineering, National Technical University of Athens, Athens 10682, Greece.

IEEE Log Number 9205465.

II. MODE CHARACTERISTICS OF THE MICROSTRIP

The geometry of the discontinuity problem under discussion is shown in Fig. 1. The step discontinuity is located at the $z = 0$ plane. The shielding box height and width are denoted by h and $2L$, respectively. Also the substrate dielectric constant and thickness are denoted by ϵ_r and d respectively

The conductive strip widths in the $z < 0$ and $z > 0$ regions are shown as $2t_1$ and $2t_2$ respectively, while ϵ denotes the axial displacement of the two microstrip lines on the $z = 0$ interface plane. Of course, the displacement of the two shielding boxes leads to an artificial geometry. However, it does not really affect the microstrip discontinuity itself, taking into account that this displacement is negligible compared to the shielding boxes' dimensions. Furthermore, a geometry where the shielding box is sufficiently wider than the microstrip is almost equivalent to the open microstrip asymmetric step discontinuity.

Because of the partial dielectric filling of the shielding box, only hybrid modes can be guided. The basic approach employed in the present analysis is the analytical technique developed by Mittra and Itoh [13] to determine the properties of both propagating and higher order evanescent modes. In [13] only even hybrid modes have been taken into account, while the asymmetric nature of the step discontinuity under study involves the properties of both odd and even modes. In the present analysis, the same notation as in [13], [14] is adopted.

In the odd mode case, the TM and TE field components are derived from the scalar potentials $\psi_i^{(e)}, \psi_i^{(h)}$ as follows:

$$\begin{aligned}
\psi_1^{(e)} &= \sum_{n=1}^{\infty} A_n^{(e)} \sinh \\
&\quad \cdot \alpha_n^{(1)} y \sin(\hat{k}_n x) \\
\psi_2^{(e)} &= \sum_{n=1}^{\infty} B_n^{(e)} \sinh \\
&\quad \cdot \alpha_n^{(2)} (h - y) \sin(\hat{k}_n x) \\
\psi_1^{(h)} &= \sum_{n=1}^{\infty} A_n^{(h)} \cosh \\
&\quad \cdot \alpha_n^{(1)} y \cos(\hat{k}_n x) \\
\psi_2^{(h)} &= \sum_{n=1}^{\infty} B_n^{(h)} \cosh \\
&\quad \cdot \alpha_n^{(2)} (h - y) \cos(\hat{k}_n x) \qquad (1)
\end{aligned}$$

where the superscripts $(e), (h)$ are associated with E (TM) and H (TE) fields respectively, while the subscript $i = 1, 2$ designates the